Strong water-mediated friction asymmetry and surface dynamics of zwitterionic solids at ambient conditions: L-alanine as a case study

J. J. Segura, A. Verdaguer, L. Garzón, E. Barrena, C. Ocal et al.

Citation: J. Chem. Phys. **134**, 124705 (2011); doi: 10.1063/1.3571453

View online: http://dx.doi.org/10.1063/1.3571453

View Table of Contents: http://jcp.aip.org/resource/1/JCPSA6/v134/i12

Published by the American Institute of Physics.

Strong water-mediated friction asymmetry and surface dynamics of zwitterionic solids at ambient conditions: L-alanine as a case study

J. J. Segura,[1] A. Verdaguer,[1] L. Garzón,[2] E. Barrena,[2] C. Ocal,[2,a)] and J. Fraxedas[1,b)]
[1]*Centre d' Investigació en Nanociència i Nanotecnologia, CIN2(CSIC-ICN), Edifici CM-7, Esfera UAB, Campus de la UAB, E-08193, Bellaterra, Spain*
[2]*Institut de Ciència de Materials de Barcelona, ICMAB-CSIC, Campus de la UAB, E-08193, Bellaterra, Spain*

(Received 26 January 2011; accepted 8 March 2011; published online 28 March 2011)

Water molecules strongly interact with freshly cleaved (011) surfaces of L-alanine single crystals at low relative humidity (below 10%) promoting diffusion of L-alanine molecules. Species mobility is enhanced above ~40% leading to the formation of two-dimensional islands with long-range order through Ostwald ripening. Scanning force microscopy experiments reveal that both, islands and terraces, are identical in nature (composition and crystallographic structure) but a relevant friction asymmetry appearing upon water–surface interaction evidences that orientation dependent properties exist between them at the molecular level. We interpret this observation as due to water incorporation in the topmost surface crystal structure. Eventually, for high humidity values, surface dissolution and roughening occur. © *2011 American Institute of Physics*. [doi:10.1063/1.3571453]

I. INTRODUCTION

The study of the interaction of water with solid surfaces at ambient conditions is of paramount importance since water–solid interfaces are involved in a myriad of relevant phenomena such as adhesion, friction, charge transport, dissolution, oxidation, chemical reactivity, etc.[1–6] Most of such everyday phenomena rely on the nanometer scale, a fact that might be surprising at first sight due to our macroscopic perception of our surroundings. However, such dimensions have been experimentally determined with different techniques such as ellipsometry,[7] infrared spectroscopy,[8] scanning probe microscopy (SPM),[9] and photoelectron spectroscopy,[10] as well as simulated by computational methods.[11]

Many surfaces of different materials with different affinity to water have been studied using different techniques.[7,9,12–20] Except for hydrophobic surfaces, above roughly 30% relative humidity (RH) (Ref. 21) many interesting phenomena arise, which might be related to the formation of a water monolayer. In the case of NaCl(001) surfaces, it has been recently shown that the charge state is correlated with the ionic mobility, which is efficiently triggered above 35%.[22] SPM investigations on gold have shown that 0.2 nm high water islands grow from the steps at 35% RH, while full coverage is achieved at 65% RH.[23]

Here we want to extend the study of the interaction of water with surfaces to materials formed by molecules relevant for life. We will concentrate on amino acids, the building blocks of proteins, and in particular on L-alanine [(S)2-aminopropanoic acid]. Amino acids are organic molecules that share a common structure made of a positively charged ammonium group (NH_3^+) and a negatively charged carboxylated group (COO^-), linked to a carbon atom and to a radical group that varies from one amino acid to another (a methyl group in the case of L-alanine). This charged structure is known as the zwitterionic form of the amino acid. The coexistence of the NH_3^+ and the COO^- hydrophilic groups and the hydrophobic methyl group makes the hydration effects in L-alanine a rather complex phenomenon that has received considerable interest in recent years, mainly from the theoretical point of view.[24–28] Although many studies, both experimental and theoretical, have been performed to shed some light to the complex role of water on protein biochemistry,[29–37] an important lack of fundamental information about the interaction of water with amino acids still exists, which can be in part overcome by investigating well characterized surfaces of crystals under humidity conditions.

From the physical properties point of view, the tribological response of organic surfaces under diverse humidity conditions becomes an obvious subject of interest by itself. A powerful tool to understand different dissipation mechanisms at surfaces is the scanning force microscope (SFM) in its lateral force imaging mode (also known as friction force microscopy, FFM).[38,39] In particular, surface characteristics influencing the frictional properties can help visualizing regions of different nature (chemical composition, structural order). However, well designed and sensitive FFM measurements can provide structural information such as molecular tilt angles and/or tilt angle azimuths. This would be, for instance, the case of observing friction anisotropy or friction asymmetry, both of them related to the dependence of friction with the sliding direction. The term friction anisotropy in general refers to the variation of friction with the relative orientation angle between sliding surfaces and is commonly correlated with surface crystallographic orientations with respect to the sliding direction (azimuth dependence). A nonisotropic structure or surface packing would, for instance, produce such an effect.[40–43] On the other hand, friction asymmetry refers to a change in friction, for the same surface symmetry

a)Electronic mail: cocal@icmab.es.
b)Electronic mail: jordi.fraxedas@cin2.es.

relationship, when the sliding direction is changed by 180°. This effect can be observed, for instance, if a molecular tilt out of the surface plane exists, being the sliding direction parallel or antiparallel to the tilt angle direction depending on the scan direction.[40] FFM has been successfully employed in organic self-assembled monolayers (SAMs) not only to discriminate between ordered configurations presenting different friction coefficients[44] or different packing[43] but also to decipher between equivalent structural domains as well as to identify highly dissipative transient molecular configurations during phase transitions.[45]

In this work, we have studied the role of water in the hydrophilic (011) surface of L-alanine crystals under controlled ambient conditions (room temperature and variable RH), by employing different scanning probe microscopies in a combined manner.

II. EXPERIMENTAL

Single crystals of L-alanine were prepared by dissolving as-received commercial powder (Fluka, nominal purity 99.5%) in Milli-Q water. The alanine-water dissolution was heated to 40°C and then cooled to room temperature with a temperature ramp of -1.5×10^{-3} °C h^{-1}, without any buffer solution.[46] With this method, crystals with long dimensions in the 0.5–2 cm range are obtained.[47]

SFM experiments were carried out at room temperature using two different instruments. One of them is a commercial 5500 Agilent Technologies SFM (Agilent Technologies, Santa Clara, CA), which is located in a glovebox in order to control humidity. RH inside the box was controlled, with an accuracy of ±5%, by flowing dry nitrogen in order to decrease RH or by bubbling nitrogen through Milli-Q water to increase RH. Freshly cleaved (011) surfaces were obtained inside the glovebox at RH ∼ 5% and *in situ* transferred to the SFM holder. Topographic and lateral force images were obtained in acoustic (*tapping*) and contact modes using microfabricated silicon cantilevers (NanoAndMore, Darmstadt, Germany) with force constants $k_c \sim 45$ N m^{-1} for tapping mode (PPP-NCHR) and $k_c \sim 0.05$ N m^{-1} (PPP-CONTR) for contact mode. Electrostatic mode images were obtained using platinum coated microfabricated silicon cantilevers (PPP-CONTPt) with $k_c \sim 0.05$ N m^{-1}.

A second setup was used to accurately cross-check the lateral force measurements at 2% < RH < 50%. This instrument is a homemade microscope head[48] combined with an SPM100 control unit and software from Nanotec Electrónica.[49] Sharpened Si_3Ni_4 tips mounted in $k_c \sim 0.1$ N m^{-1} cantilevers were used (Veeco, Mannheim, Germany).

In contact mode measurements, normal and torsion deflections of the cantilever were simultaneously measured by means of a four-quadrant photodiode. The voltage difference of the upper and lower segments is proportional to the normal deflection of the cantilever and consequently related to the sample topography. The voltage range between the right and the left segments is proportional to the torsion of the cantilever which is a direct measure of the lateral force and related to friction if the fast-scan direction is set orthogonal to the cantilever axis. Provided the lateral force always opposes the tip motion, the tip twist reverses when the scan direction is inverted and the complete friction loop consists of a forward (left to right) and a backward (right to left) scans. The local frictional response is defined as $1/2(F_{lf} - F_{lb})$ where F_{li} is the lateral force signal along that line in the forward (i=f) and backward (i=b) scan.

III. RESULTS AND DISCUSSION

A. Surface dynamics

The room temperature crystal structure of L-alanine is orthorhombic (space group $P2_12_12_1$) and lattice parameters $a = 0.603$ nm, $b = 1.234$ nm, and $c = 0.578$ nm.[50] Figure 1 shows the top (a) and side (b) view projections of the (011) surface. The surface unit cell parameters are 0.603 and 1.36 nm (along and perpendicular to the *a*-axis, respectively) as indicated in Fig. 1(a). The molecular density is ≃ 4.87 molecules nm^{-2}, i.e., the area per molecule is about 20.5 $Å^2$. Note that the L-alanine molecules adopt a *standing up* configuration within the surface and the separation between adjacent molecular planes is 0.52 nm [Fig. 1(b)].

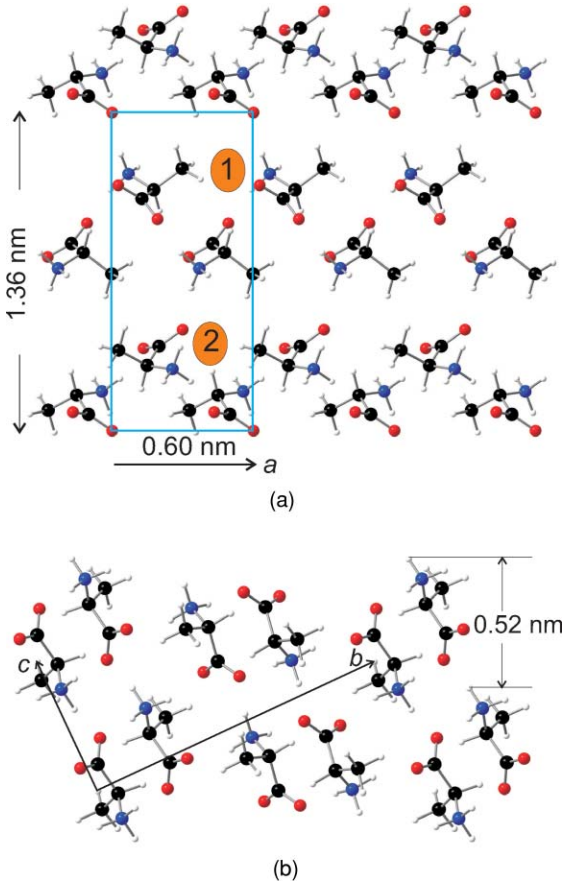

FIG. 1. (a) Top and (b) side views of the (011) crystal face of L-alanine projected across and along the *a*-axis, respectively. The room temperature crystal structure is orthorhombic, space group $P2_12_12_1$, with four molecules per unit cell and cell parameters $a = 0.6032$, $b = 1.2343$, and $c = 0.5784$ nm. Crystallographic data taken from Lehmann *et al.* (Ref. 50). Carbon, oxygen, nitrogen, and hydrogen atoms are represented by black, red, blue, and white spheres, respectively. The surface unit cell, in blue in (a), is 0.60×1.36 nm^2.

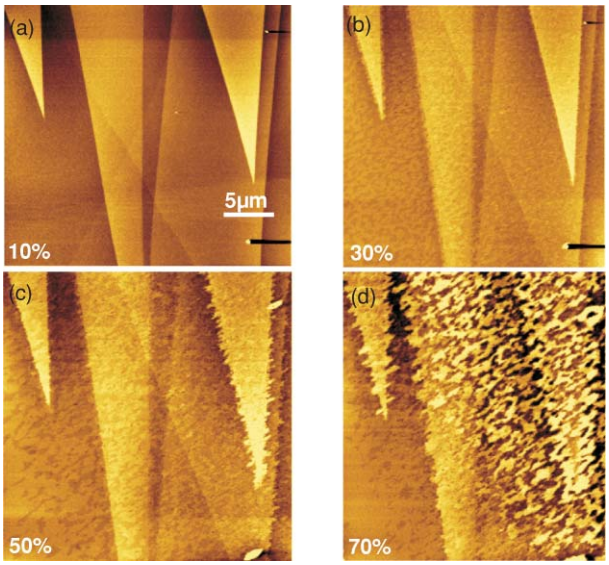

FIG. 2. Topographic SFM images of a (011) surface of a L-alanine single crystal. The images were acquired on freshly cleaved surfaces in the acoustic (tapping) operation mode in a glovebox at room temperature and at the RHs: (a) 10%, (b) 30%, (c) 50%, and (d) 70%. Cleavage was performed at RH $\sim$ 5%. Scale is 30 μm $\times$ 30 μm.

Figure 2 shows tapping mode topographic images of a (011) surface cleaved at RH $\sim$ 5% and taken at different RHs. Cleavage induces the formation of triangular- or V-shaped terraces, with extremely long step edges (several tens of micrometers) forming acute angles between 5° and 30°. Note the presence of underlying X-shaped slip traces in Fig. 2(a). Similar step structures have been reported for cleavage surfaces of different single crystals such as CaF_2,[51] BaF_2,[52] and mono clinic L-arginine phosphate monohydrate.[53] The measured step heights are integer multiples of $\simeq$ 0.5 nm, which corresponds to the distance between two adjacent (011) molecular planes [see Fig. 1(b)]. Already at RH $\sim$ 10%, a non-negligible surface roughness is observed, indicating the proclivity of water to induce surface modifications. Conversely to what is expected from an interaction activated at defects, both step edges and terraces are equally perturbed for a wide range of humidities, pointing to a mechanism involving incorporation of water to the crystal surface. With increasing RH the surface becomes strongly perturbed [see Figs. 2(b) and 2(c)] and above $\sim$ 50% RH the perturbation is so strong that in some regions the initial step structure becomes hardly recognisable [Fig. 2(d)]. Indeed, for increasing RH values, the influence of the tip becomes more relevant, but important perturbation induced by the sweeping action of the tip is discarded since surface roughening was observed as well in regions of the surface that were not previously scanned. Consequently, the process reported here is mainly induced by water.[47]

Figure 3(a) shows, at larger magnification, the evolution of the surface after being exposed to $\sim$25 and $\sim$40% RH. The initial scenario consisting of flat regions (terraces) separated by steps has evolved as to reveal two important points that will be addressed in detail next: (i) each region exhibits now two well differentiated levels, terraces, and islands. The measured islands' heights are $\sim$0.35 nm, clearly smaller than the distance between adjacent (011) molecular planes ($\sim$0.5 nm), a clear indication of the restructuration of the surface induced by water. (ii) The islands' size is much larger for the higher RH, suggesting a coarsening process in which both increasing humidity and elapsed time play a joint role. Provided below $\sim$20% only small changes in island evolution are observed after several hours, we illustrate the coarsening process for a given humidity as a function of time with data obtained at $\sim$40% [Fig. 3(b)]. At this RH the effects induced by water are quite evident in a reasonable time scale (few hours). Quick inspection of the images clearly reveals that larger islands grow at the expense of smaller ones, a well-known phenomenon termed (2D) Ostwald ripening.[54–56]

Due to the difficulty of tracking individual islands as they evolve, we instead compare the total area covered by islands and the corresponding area to perimeter ratio, as shown in Fig. 3(c). In order to understand the role and influence of RH in the process, the recorded glovebox humidity is also shown (continuous blue line). It displays a slow increase up to a constant value kept at 40%. This RH value can be regarded as a threshold dividing the plot into two clearly differentiated regions. The area to perimeter ratio is constant only below the stabilization of RH and it increases almost monotonically from there on. This first result indicates that below such a threshold the small islands formed at the beginning are essentially stable but above it the islands coalescence building larger islands. On the other hand, the covered area remains quite constant (slightly above 50% of the total explored surface) over the entire experiment and basically equal to the area of the islands formed from cleavage to acquisition of the first image at the lower RH. This second result supports the existence of a process where water strongly interacts, likely incorporated into the surface at low humidity. Surface diffusion seems to be relatively moderate until an increase in humidity provides an extra mobility to the surface species triggering the Ostwald ripening process. As it will be discussed later on, this threshold RH seems to have a crucial role leading to an unexpected increase in friction asymmetry, supporting our interpretation of an increase in mobility. Observation by SFM of Ostwald ripening induced on a surface by adsorbed water films has been already reported for salt nanocrystals deposited on silicon oxide substrates[57] and for boric acid surfaces.[58]

As already seen [Fig. 2(d)], for RH well above 40% surface disruption becomes evident. This is exemplified in Fig. 4, where the evolution from 50% up to 80% is shown. Already at 50% the species mobility is so high that Ostwald ripening leads to the formation of large terraces with rounded edges and embedded voids, reminiscent of pre-existing islands and the empty space between them. As humidity keeps rising, an enhanced molecular diffusion permits minimizing the surface area by filling the holes (surface healing), reducing hills (i.e., species diffusion is no longer strictly 2D), and smoothing the terraces' edges in a way that the surface topography becomes hardly distinguishable from the original surface. A change in mass transport mechanism from 2D to 3D is evident when even higher humidity is reached (between 70% and 80%). The step edges start to roughen and eventually new holes appear at the terraces. Conversely to the mechanism commented above for low RH, under severe humidity conditions

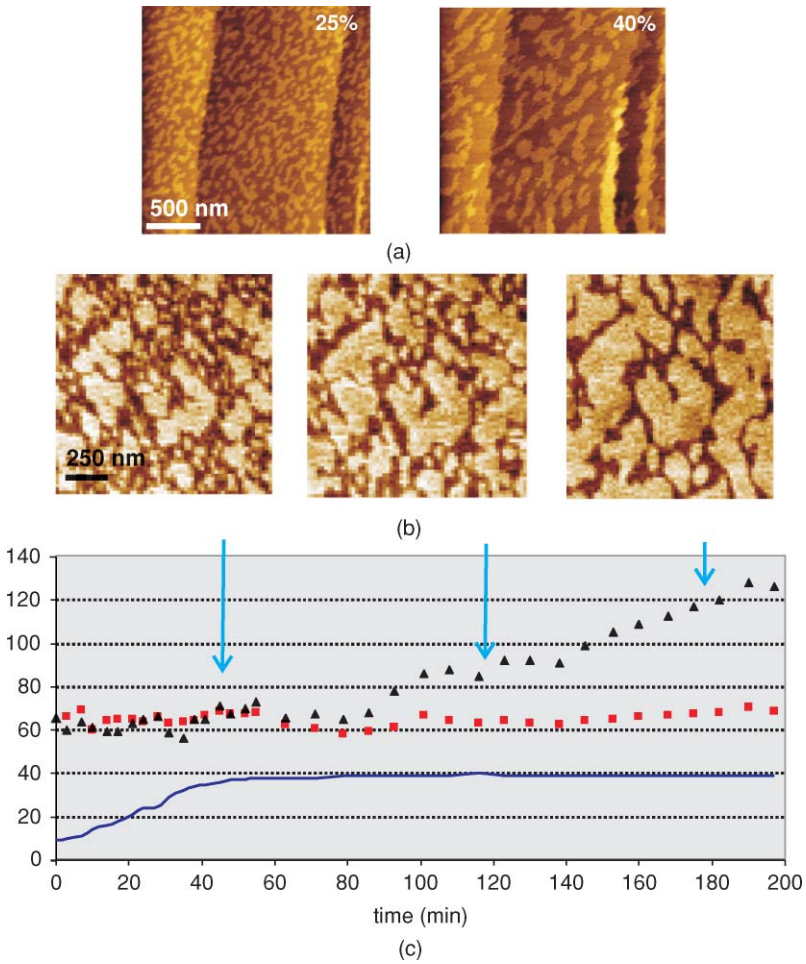

FIG. 3. (a) Topographic SFM images of a (011) surface of a L-alanine single crystal. The images were acquired on freshly cleaved surfaces in the acoustic (tapping) operation mode in a glovebox at room temperature and at RHs: (left) ~ 25% and (right) ~ 40%. Cleavage was performed at RH ~ 5%. (b) Time evolution of SFM images evidencing Ostwald ripening taken at RH ~ 40%. (c) Time evolution of the area fraction (in %, red squares), the area to perimeter ratio (black triangles), and RH (blue continuous line). The time where the images from (b) were taken is indicated by blue arrows.

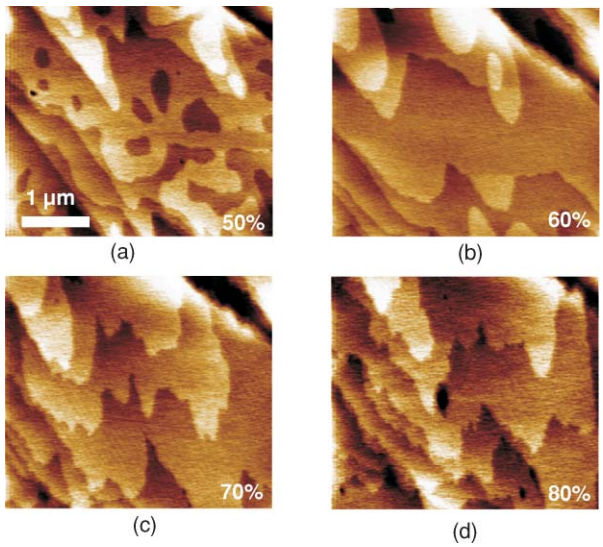

FIG. 4. Topographic SFM images of a (011) surface of a L-alanine single crystal. The images were acquired on freshly cleaved surfaces in the acoustic (tapping) operation mode in a glovebox at room temperature and at RHs: (a) 50%, (b) 60%, (c) 70%, and (d) 80%. Cleavage was performed at RH ~ 5%.

a true roughening occurs and the surface becomes dissolved. This process is surely enhanced by the influence of the tip, but real time visualization of surface diffusion evidences that dissolution takes place with no correlation with the scanning direction.

B. Friction asymmetry

All water-induced processes described above (water incorporation, species diffusion, Ostwald ripening, and roughening) involve molecular displacements and rearrangements where a large number of degrees of freedom significantly contribute to energy dissipation. Because lateral force imaging is especially useful to get insight on the dissipation mechanisms occurring at surfaces, in the following we describe results obtained by this technique. Figure 5(a) shows topography (left) and forward lateral force (right) images taken in contact mode at room temperature and 40% RH. The topographic image shows the already described two-level distribution and the lateral force image reveals clear contrast between them, with the islands exhibiting a higher (brighter in color scale) forward lateral force. Note that lateral force signals are measured as a result of the cantilever torsion, hence having an opposite

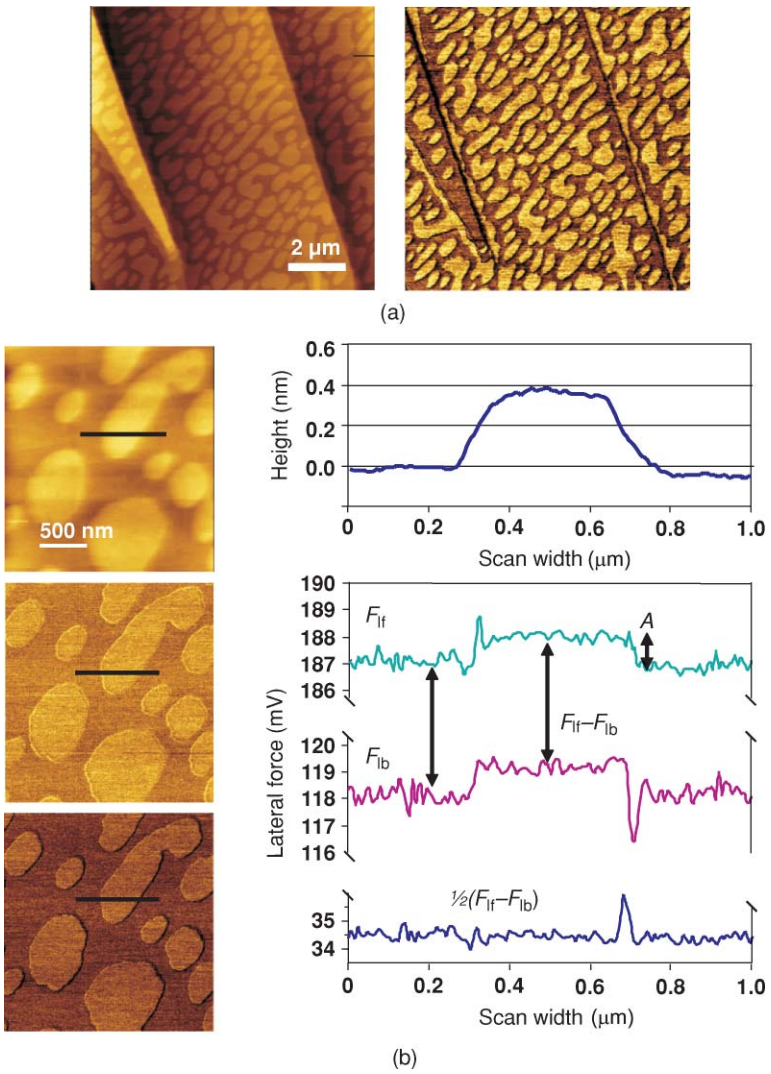

FIG. 5. (a) Topography (left) and lateral force (right) images taken in contact mode at room temperature and 40% RH. Scale is 11 μm × 11 μm. (b) Topography (top left), forward scan lateral force (middle left), and backward scan lateral force (bottom left) images taken at room temperature and 40% RH. The corresponding cross section profiles are shown to the right. *A* stands for the friction asymmetry while F_{lf} and F_{lb} represent the lateral force signals along the forward and backward scan directions, respectively. The total friction is calculated as $1/2(F_{lf} - F_{lb})$.

sign for reversed scan directions, i.e., larger lateral forces are visualized as bright colors in the forward scans but as dark colors in the backward path. Consequently, opposite image contrast must be recorded if surface regions of different friction coexist, as for the case of chemically differentiated regions. In Fig. 5(b) simultaneous topography (top left), forward (middle left) and backward (bottom left) lateral force images taken at room temperature and 40% RH are shown. Taking the terrace level as *in situ* reference in the corresponding topographic profile, the islands' height is 0.35 nm. Interestingly, lateral force imaging reveals that the islands appear brighter than the terrace in both scan directions. This result means that the lateral force is asymmetric, i.e., the cantilever lateral torsion changes within each region when the sliding direction is reversed (180°). On the other hand, the same difference in cantilever torsion magnitude (A in the profiles) between islands and terrace is measured. More specifically, friction calculated as $1/2(F_{lf} - F_{lb})$ (bottom of line profiles) reveals that an equal value (same friction coefficient) is obtained on islands and terrace, as otherwise characteristic of areas of homogeneous surface properties and, in particular, same chemical composition. Note that this effect is observed, except at the islands' boundaries where cantilever torsion is influenced by the topographic change, independently of the area of the islands, discarding size effects.

A similar asymmetric effect has been reported for organic ferroelectric crystals,[59] lipid monolayers on mica,[40] alkanethiol SAMs domains on gold,[43] and for cleavage surfaces of alkaline earth sulfate crystals.[60] The origin is an asymmetric tip–surface interaction potential (illustrated by a saw-tooth-like potential by Bluhm *et al.*[59]) ascribed either to domains with the same structure but opposite molecular tilt directions or to alternate terraces with a mirror plane surface structure. Islands and terraces of Fig. 5 can be visualized as such surface domains and in the following we will focus on the origin of their asymmetry in terms of friction. In order to exclude electrostatic interaction as the origin of the frictional asymmetry (asymmetric contact potential difference), scanning polarization force microscopy (SPFM) combined with Kelvin probe force microscopy

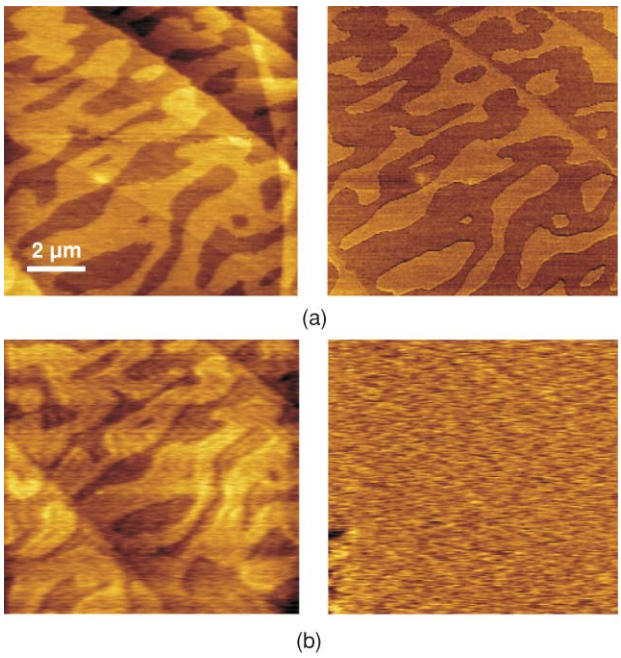

FIG. 6. (a) Topography (left) and lateral force (right) contact mode images and (b) SPFM (left) and KPFM (right) images of (011) surfaces of L-alanine taken at 50% RH.

(KPFM) measurements are presented (Fig. 6). SPFM gives topographic information of the surface modulated by the surface dielectric properties while KPFM gives information on the dipolar and charge distribution on the surface.[61,62] Figure 6(a) shows contact mode topographic (left) and lateral force (right) images of a (011) surface taken at 50% RH where the two regions corresponding to terraces and islands can be identified and Fig. 6(b) shows SPFM (left) and KPFM (right) images of the same region. SPFM topographic images show the same topography features and same height values (within experimental error) as observed in contact mode, indicating that no dielectric differences exist between islands and terraces. Similarly, a featureless KPFM image implies the existence of a unique surface contact potential in both regions, supporting once more their same chemical nature.

In Fig. 7(b) the friction asymmetry is represented as a function of the sample orientation θ while keeping the scan direction fixed [see Fig. 7(a)]. The 180° periodicity reveals that both friction asymmetry and anisotropy simultaneously exist. The analysis as a function of RH is also presented in Fig. 7(c). It turns out that the observed friction asymmetry is dependent on RH with a maximum at $\sim$ 40%, in agreement with the triggering value of enhanced surface species mobility (Fig. 3), and falls back to the lowest detectable value after removal of water vapor. This fact points to a possible reversible incorporation of water within the surface (see below).

Altogether, the above results indicate that ascribing friction asymmetry to an asymmetric (180° rotated) molecular structure of islands and terraces is adequate and this can be best explored with high resolution SFM. Figure 8 shows a molecular resolution image of a surface obtained after exposure to 40% RH over an area including part of one terrace and part of one island. Resolution is high enough to show molecular order in both regions, with $\sim$ 1.6 nm separated rows running along a common crystallographic direction. Even though the observation of a unique 2D order supports our interpretation, regretfully, resolution does not reach the level needed to distinguish molecular positions within the surface unit cell.

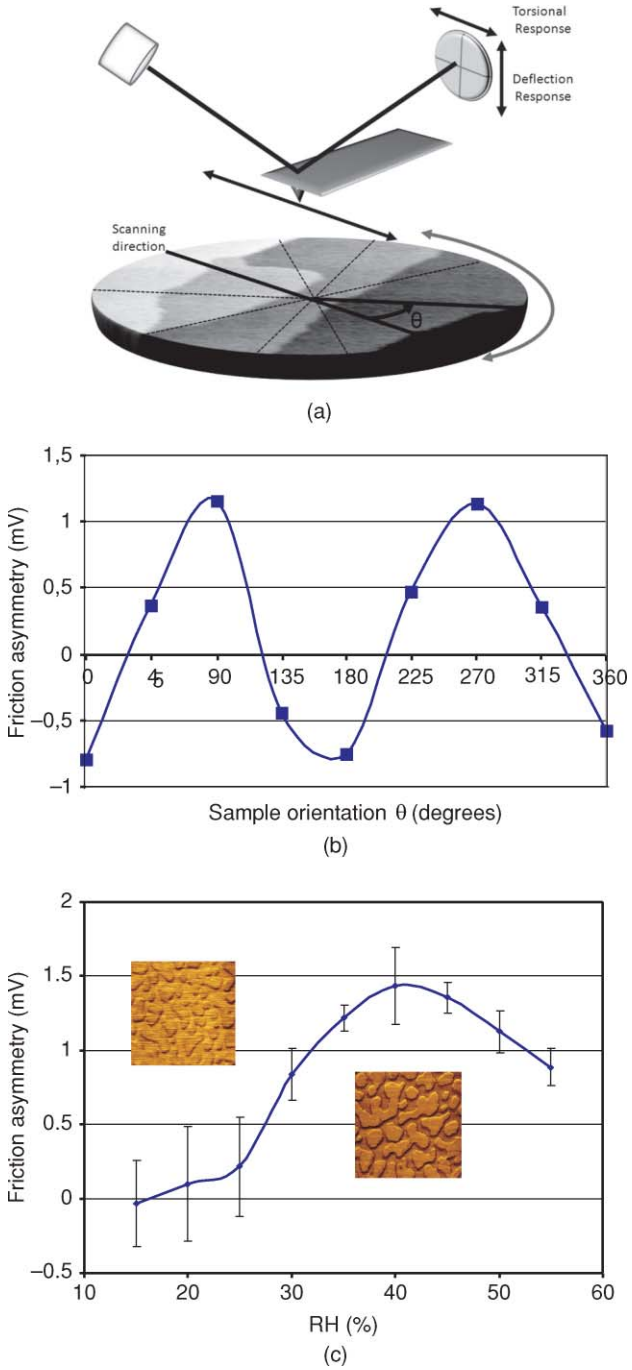

FIG. 7. (a) Scheme showing the cantilever scanning direction and sample orientation (θ) with regard to the torsional and deflection responses in the four-sectors detector. (b) Friction asymmetry as a function of θ with respect to the forward scan direction. (c) Friction asymmetry as a function of RH. Selected lateral force images corresponding to $\sim$ 20 and 40% RH are displayed. The lines in (b) and (c) are guides to the eye.

C. Structural model

Before proposing a structural model we summarize the information at hand. As the product of water–surface interac-

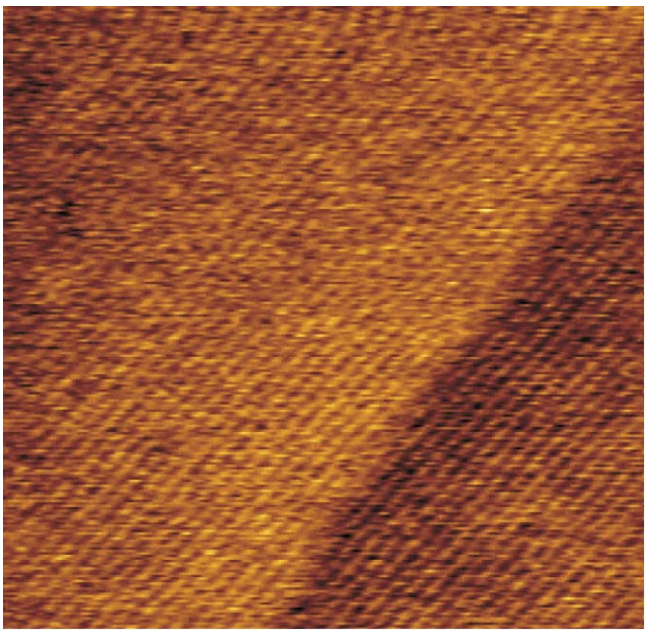

FIG. 8. High resolution topographic image (100 nm × 100 nm) of a terrace and an island, taken in contact mode after exposure to the sample to 40% RH.

tion, 0.35 nm high islands develop on the surface terraces at moderate RH. Both, islands and terraces, have the same chemical composition, exhibit rectangular 2D order with the large dimension equal to 1.6 nm and a high friction asymmetry with no differences in dipole orientation. These two levels must be mirrorlike symmetric and should have a lower molecular density than the (011) initial surface. This scenario is compatible with a 2D surface ordering in which the molecular species at the exposed surface are ordered in a *lying flat* arrangement with *pm* rectangular symmetry in which water molecules are importantly involved.

In pure single component surfaces, usually dense molecular packing sterically prevents many of the possible modes of energy dissipation such as rotational motions or molecular bending, otherwise more probable at open molecular structures. On the other hand, it is known that 2D arrangements different than those corresponding to ideal (bulk terminated) surface planes, known as reconstructions, can be stabilized at surfaces. The reasons for the appearance of such surface reconstructions are diverse but strong interaction with gas or liquid molecules are usual triggers of surface species reordering. Eventually, the final surface is that minimizing the surface energy for specific environmental conditions. One way or the other, a reduction of molecular density at surfaces may certainly result in an enhancement of possible dissipation routes as observed here. Instead of hypothesizing a completely new 2D molecular structure as responsible for the results reported here, we judge worth to evaluate the viability of specific packings already existing in L-alanine crystal planes with the aim of searching for possible structural models.

The stripelike structure observed in Fig. 8 reminds that observed for the (120) plane. High resolution images taken on (120) cleavage surfaces (not shown) reveal parallel molecular chains running along the crystallographic *c*-axis with a well resolved periodicity of 1.7 nm, i.e., the expected surface unit

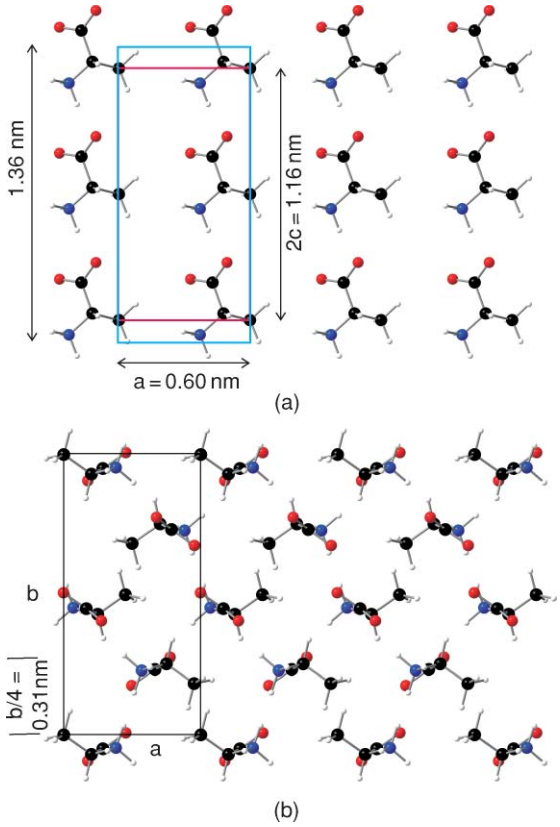

FIG. 9. (a) Top and (b) side views of the (040) crystal face of L-alanine projected along the *b*- and *c*-axis, respectively. Carbon, oxygen, nitrogen, and hydrogen atoms are represented by black, red, blue, and white spheres, respectively. The surface unit cell, $a \times 2c = 0.60 \times 1.16$ nm^2 (red), is compared to that from (011) shown in Fig. 1(a), 0.60×1.36 nm^2 (blue).

cell for the ideal (120) surface and coinciding with previous SFM results.[63] Though this periodicity agrees reasonably with the in-plane separation between rows in Fig. 8, the inter-plane separation is 0.43 nm, clearly larger than the measured islands height. Moreover, a molecular density of 4 molecules nm^{-2} is too close to that of the (011) to justify the observed two levels landscape.

A more appropriate molecular packing, able to match with the surface symmetry of the initial (011) surface, and consisting of a planar arrangement of molecules, is presented in Fig. 9. This structure corresponds to the (040) crystal plane with a surface unit cell of 0.603 nm × 0.578 nm, along the *a*- and *c*-crystallographic axis, respectively, i.e., it perfectly matches with the (011) plane in one direction. The reduced unit cell of the (011) plane [see Fig. 1(a)] has been drawn in Fig. 9(a) to illustrate that the uniaxial mismatch between both planes is adequate so that two lying molecules in an arrangement as that of the (040) plane would perfectly match on the fourfold positions [labelled 1, 2 in Fig. 1(a)] of the underlying (011)-terminated crystal. With a density of ~ 2.9 molecules nm^{-2}, this packing is consistent with the formation of two levels out of one initial much denser (011) surface (~ 4.9 molecules nm^{-2}). In terms of friction, such an open 2D structure with a large area per molecule (34.8 Å^2 vs 20.5 Å^2) would favor molecular motions responsible for large dissipation processes. The friction asymmetry between

islands and terraces may be explained via the uniaxial mismatch and the unique molecular orientation within the surface plane, which makes equally probable the formation of 180° rotated domains. Finally, a good estimation for the expected thickness of this planar arrangement is the distance between adjacent (040) planes, which is $b/4 \sim 0.31$ nm [Fig. 9(b)], very close to the observed islands' height. In addition, a lying down surface molecular distribution supports a hydrophobic character since the molecular dipoles lie nearly parallel to the surface.[47]

How credible is the water-mediated formation of a surface as the model proposed here? The high affinity to water exhibited by the (011) surface, which is experimentally observed at low RH values and has been previously interpreted in terms of nearly collinear alanine dipole–water dipole interactions,[47] may lead to the dissociation of the L-alanine intermolecular bonds. In crystals L-alanine molecules are bound together through N-H. . .O hydrogen bonds between the ammonium and carboxylic groups of nearest molecules. Water molecules may break such bonds and solvate the individual molecules through N-H. . .O and O. . .H-O hydrogen bonds. The solvated zwitterionic form of L-alanine can differ significantly from the crystalline phase but has been found to be stable.[27] However, the solvated system cannot stand the whole set of molecules at the same terrace level and some are liberated to the surface. They would diffuse and nucleate in islands adopting a lying down configuration to optimize van der Waals interactions and growing by Ostwald ripening to reduce surface energy. On the other hand, molecular removal would cause a relaxation of the now less dense terrace level in such a way that the remaining molecules are able to bend and eventually, for a low enough density, arrange in a lying down configuration as well. If approximately one out of two L-alanine molecules is displaced during solvation, islands will cover $\sim 50\%$ of the terraces (or a bit more if water is incorporated), in good agreement with Fig. 3(c). For energetic reasons, both levels must be equivalent domains. Their expected tension-free hydrated structure is presumably uniaxially strained to match the underlying (011) lattice, providing an appropriate 180° surface asymmetry. At this stage, with the molecular dipoles parallel to the surface in both levels, the strength of the dipolar interactions is reduced and the initial hydrophilic character turns into hydrophobic. Interestingly, this hydrophobicity is reinforced by the incorporation of water.

IV. CONCLUSIONS

We have studied the interaction of water with freshly cleaved (011) surfaces of L-alanine single crystals as a function of RH combining different SFM techniques, both in contact and noncontact operational modes (lateral force, molecular resolution contact mode, and electrostatic modes). We have shown that water molecules strongly interact with the initial hydrophilic (011) surface even at low relative humidities ($RH < 10\%$), promoting diffusion of L-alanine molecules and creating a two level landscape formed by terraces and islands that undergo 2D Ostwald ripening. The two surface levels exhibit the same nature and crystallographic structure but a 180° rotated orientation as revealed by lateral force and supported by high resolution SFM images. Though our molecular resolution images do not permit elucidating the actual newly generated structure, a structural model based on energetic and geometric arguments is presented in which molecules lie flat in a low density ordered arrangement uniaxially matching with the underlying (011) crystal orientation.

The reported water-mediated surface reorganization can be seen as a surface self-passivation process with a switchable response, as revealed by the friction response as a function of RH, with promising implications in the investigation field of biomolecules. Although our findings apply to the particular case of L-alanine, they are foreseen of relevance for understanding the complex interplay of biomolecules, such as proteins, with water, i.e., protein hydration, essential for their three-dimensional structure and activity.

ACKNOWLEDGMENTS

This work was supported by the Ministerio de Ciencia y Tecnología (Spain), through projects FIS2009-08355, MAT2010-20020, and CONSOLIDER CSD2007-00041 (NANOSELECT) and by the Generalitat de Catalunya (SGR 00909). J.J.S. thanks the Consejo Superior de Investigaciones Científicas (CSIC) for a JAE DOC PhD grant and A.V. acknowledges support from the Spanish Ramón y Cajal Program.

[1] J. N. Israelachvili, *Intermolecular and Surface Forces* (Academic, London, 1991).
[2] P. A. Thiel and T. E. Madey, Surf. Sci. Rep. **7**, 211 (1987).
[3] M. A. Henderson, Surf. Sci. Rep. **46**, 1 (2002).
[4] B. J. Finlayson-Pitts, Chem. Rev. **103**, 4801 (2003).
[5] A. Verdaguer, G. M. Sacha, H. Bluhm, and M. Salmeron, Chem. Rev. **106**, 1478 (2006).
[6] A. Hodgson and S. Haq, Surf. Sci. Rep. **64**, 381 (2009).
[7] D. Beaglehole and H. K. Christenson, J. Phys. Chem. **96**, 3395 (1992).
[8] M. Foster and G. E. Ewing, J. Chem. Phys. **112**, 6817 (2000).
[9] J. Hu, X. D. Xiao, D. F. Ogletree, and M. Salmeron, Science **268**, 267 (1995).
[10] H. Bluhm, D. F. Ogletree, C. S. Fadley, Z. Hussain, and M. Salmeron, J. Phys.: Condens. Matter **14**, L227 (2002).
[11] O. Engkvist and A. J. Stone, J. Chem. Phys. **112**, 6827 (2000).
[12] W. Cantrell and G. E. Ewing, J. Phys. Chem. B **105**, 5434 (2001).
[13] T. Fukuma, Y. Ueda, S. Yoshioka, and H. Asakawa, Phys. Rev. Lett. **104**, 016101 (2010).
[14] K. Xu, P. Cao, and J. R. Heath, Science **329**, 1188 (2010).
[15] A. L. Goodman, E. T. Bernadrand, and V. H. Grassian, J. Phys. Chem. A **105**, 6443 (2001).
[16] H. A. Al-Abadleh and V. H. Grassian, Surf. Sci. Rep. **52**, 63 (2003).
[17] M. Foster, M. DAgostino, and D. Passno, Surf. Sci. **590**, 31 (2005).
[18] D. B. Asay and S. H. Kim, J. Phys. Chem. B **109**, 16760 (2005).
[19] G. E. Ewing, Chem. Rev. **106**, 1511 (2006).
[20] A. L. Summer, E. J. Menke, Y. Dubowski, J. T. Newberg, R. M. Penner, J. C. Hemminger, L. M. Wingen, T. Brauers, and B. J. Finlayson-Pitts, Phys. Chem. Chem Phys. **6**, 604 (2004).
[21] RH (in %) is defined for a given ambient temperature as the ratio between the ambient water vapor pressure and the saturated water vapor pressure at such temperature.
[22] A. Verdaguer, J. J. Segura, J. Fraxedas, H. Bluhm, and M. Salmeron, J. Phys. Chem. C **112**, 16898 (2008).
[23] A. Gil, J. Colchero, M. Luna, J. Gómez-Herrero, and A. M. Baró, Langmuir **16**, 5086 (2000).
[24] S. Park, D. Ahn, and S. Lee, Chem. Phys. Lett. **371**, 74 (2003).
[25] K. Sagarik and S. Dokmaisrijan, J. Mol. Struct.: THEOCHEM **718**, 31 (2005).

[26]A. Osted, J. Kongsted, K. V. Mikkelsen, and O. Christiansen, Chem. Phys. Lett. **429**, 430 (2006).
[27]I. Degtyarenko, K. J. Jalkanen, A. Gurtovenko, and R. M. Nieminen, J. Comput. Theor. Nanosci. **5**, 277 (2008).
[28]B. Z. Chowdhry, T. J. Dines, S. Jabeen, and R. Withnall, J. Phys. Chem. A **112**, 10333 (2008).
[29]M. F. Colombo, D. C. Ran, and V. A. Parsegian, Science **256**, 655 (1992).
[30]D. I. Svergun, S. Richard, M. H. J. Koch, Z. Sayers, S. Kuprin, and G. Zaccai, Proc. Natl. Acad. Sci. U.S.A. **95**, 2267 (1998).
[31]L. Lo Conte, C. Cothia, and J. Janin, J. Mol. Biol. **285**, 2177 (1999).
[32]V. Makarov, B. M. Pettitt, and M. Feig, Acc. Chem. Res. **35**, 376 (2002).
[33]J. Milhaud, Biochim. Biophys. Acta **1663**, 19 (2004).
[34]J. Lin, I. A. Balabin, and D. N. Beratan, Science **310**, 1311 (2005).
[35]F. Garczarek and K. Gerwert, Nature (London) **439**, 109 (2006).
[36]S. Ebbinghaus, S. J. Kim, M. Heyden, X. Yu, U. Hengen, M. Gruebele, and D. M. Leitner, Proc. Natl. Acad. Sci. U.S.A. **104**, 20749 (2007).
[37]P. Ball, Chem. Rev. **108**, 74 (2008).
[38]R. W. Carpick and M. Salmeron, Chem. Rev. **97**, 1163 (1997).
[39]M. Salmeron, S. Kopta, E. Barrena, and C. Ocal, *Fundamentals of Tribology and Bridging the Gap Between the Macro- and Micro/Nanoscales*, NATO Advanced Studies Institute, Series E: Applied Sciences, edited by B. Bhushan (Kluwer Academic, Dordrecht, 2001), Vol. **10**, pp. 41–52.
[40]M. Liley, D. Gourdon, D. Stamou, U. Meseth, T. M. Fischer, C. Lautz, H. Stahlberg, H. Vogel, N. A. Burnham, and C. Dusch, Science **280**, 273 (1998).
[41]K. Hisada and C. M. Knobler, Colloids and Surfaces A: Physicochemical and Engineering Aspects **198–200**, 21–30 (2002).
[42]J. Y. Park, D. F. Ogletree, M. Salmeron, R. A. Ribeiro, P. C. Canfield, C. J. Jenks, and P. A. Thiel, Science **309**, 1354 (2005).
[43]C. Munuera, E. Barrena, and C. Ocal, J. Phys. Chem. A **111** 12721 (2007).
[44]E. Barrena, C. Ocal, and M. Salmeron, J. Chem. Phys. **113**, 2413 (2000).
[45]C. Munuera and C. Ocal, J. Chem. Phys. **124**, 206102 (2006).
[46]C. Razzetti, M. Ardoino, L. Zanotti, M. Zha, and C. Paorici, Cryst. Res. Technol. **37**, 456 (2002).
[47]J. J. Segura, A. Verdaguer, M. Cobián, E. R. Hernández, and J. Fraxedas, J. Am. Chem. Soc. **131**, 17853 (2009).
[48]W. F. Kolbe, D. F. Ogletree, and M. Salmeron, Ultramicroscopy **42–44**, 1113 (1992).
[49]I. Horcas, R. Fernández, J. M. Gómez-Rodríguez, J. Colchero, J. Gómez-Herrero, and A. M. Baró, Rev. Sci. Instrum. **78**, 013705 (2007).
[50]M. S. Lehmann, T. F. Koetzle, and W. C. Hamilton, J. Am. Chem. Soc. **94**, 2657 (1972).
[51]J. Engelhardt, H. Dabringhaus, and K. Wandelt, Surf. Sci. **448**, 187 (2000).
[52]M. Cardellach, A. Verdaguer, J. Santiso, and J. Fraxedas, J. Chem. Phys. **132**, 234708 (2010).
[53]Y. L. Geng, D. Xu, X. Q. Wang, G. W. Yu, G. H. Zhang, and H. B. Zhang, J. Cryst. Growth **282**, 208 (2005).
[54]O. Krichevsky and J. Stavans, Phys. Rev. B **52**, 1818 (1995).
[55]D. J. Semin, A. Lo, S. E. Roark, R. T. Skodje, and K. L. Rowlen, J. Chem. Phys. **105**, 5542 (1996).
[56]H. Basagaoglu, C. T. Green, P. Meakin, and B. J. McCoy, J. Chem. Phys. **121**, 7987 (2004).
[57]K. Arima, P. Jiang, D.-S. Lin, A. Verdaguer, and M. Salmeron, J. Phys. Chem. A **113**, 9715 (2009).
[58]J. A. S. Cleaver and P. Wong, Surf. Interface Anal. **36**, 1592 (2004).
[59]H. Bluhm, U. D. Schwarz, and R. Wiesendanger, Phys. Rev. B **57**, 161 (1998).
[60]H. Shindo, K. Shitagami, T. Sugai, and S. Kondo, Phys. Chem. Chem. Phys. **1**, 1597 (1999).
[61]J. Hu, X.-D. Xiao, and M. Salmeron, Appl. Phys. Lett. **67**, 476 (1995).
[62]A. Verdaguer, M. Cardellach, J. J. Segura, G. M. Sacha, J. Moser, M. Zdrojek, A. Bachtold, and J. Fraxedas, Appl. Phys. Lett. **94**, 233105 (2009).
[63]H. M. Guo, H. W. Liu, Y. L. Wang, H. J. Gao, Y. Gong, H. Y. Jiang, and W. Q. Wang, Surf. Sci. **552**, 70 (2004).